

**Journal name:** Cellular and Molecular Life Sciences

**Article title, author names; affiliation and e-mail address of the corresponding author:**

F-ACTIN BINDING PROTEIN, ANILLIN, REGULATES INTEGRITY OF INTERCELLULAR  
JUNCTIONS IN HUMAN EPITHELIAL CELLS

Dongdong Wang<sup>1#</sup>, Gibran K. Chadha<sup>1#</sup>, Alex Feygin<sup>1</sup>, and Andrei I. Ivanov<sup>1,2,3\*</sup>

<sup>1</sup>Department of Human and Molecular Genetics, <sup>2</sup>Virginia Institute of Molecular  
Medicine, <sup>3</sup>VCU Massey Cancer Center, Virginia Commonwealth University, Richmond,  
VA 23298, USA

<sup>#</sup>These authors contributed equally to the paper.

\*Address for correspondence:

Andrei I. Ivanov

Department of Human and Molecular Genetics

Virginia Commonwealth University

Massey Cancer Center, Box 980035

401 College Street, Room 223

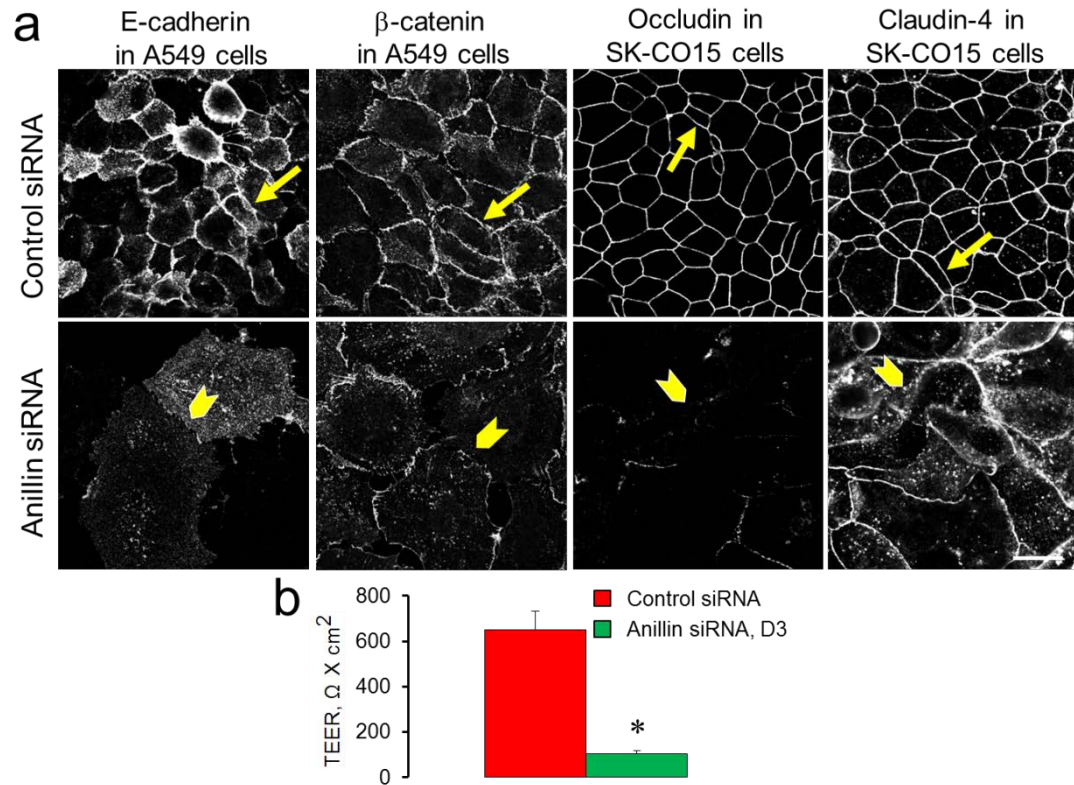
Richmond, VA 23298

Tel. (804) 628-4425

Email: aivanov2@vcu.edu

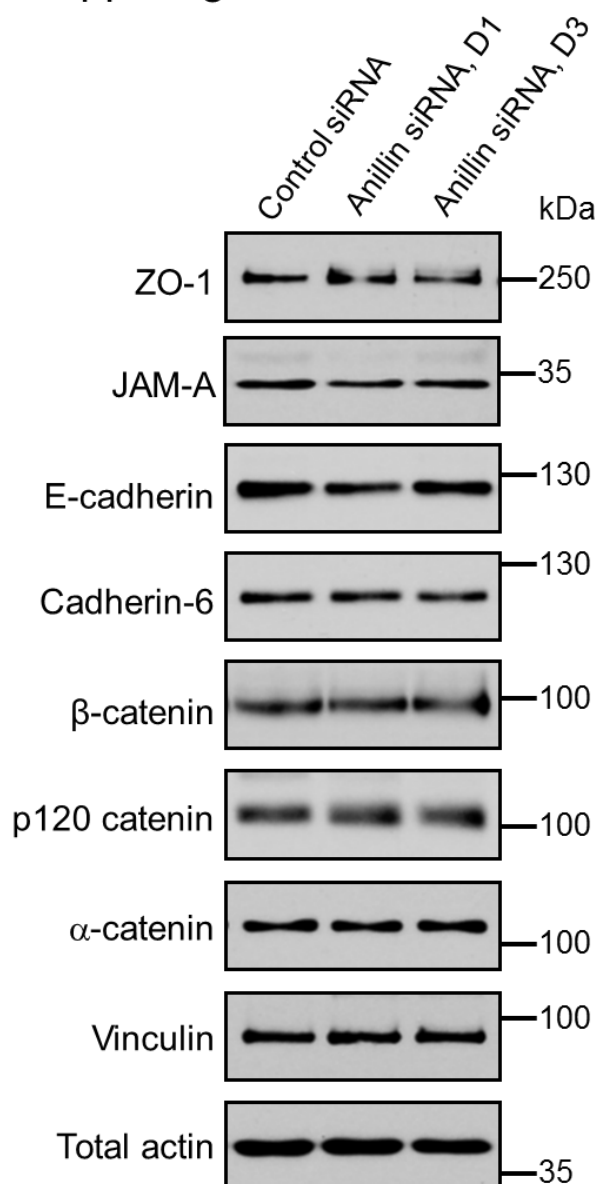
**RUNNING HEAD:** Anillin and epithelial junctions.

## Suppl. Fig. 1



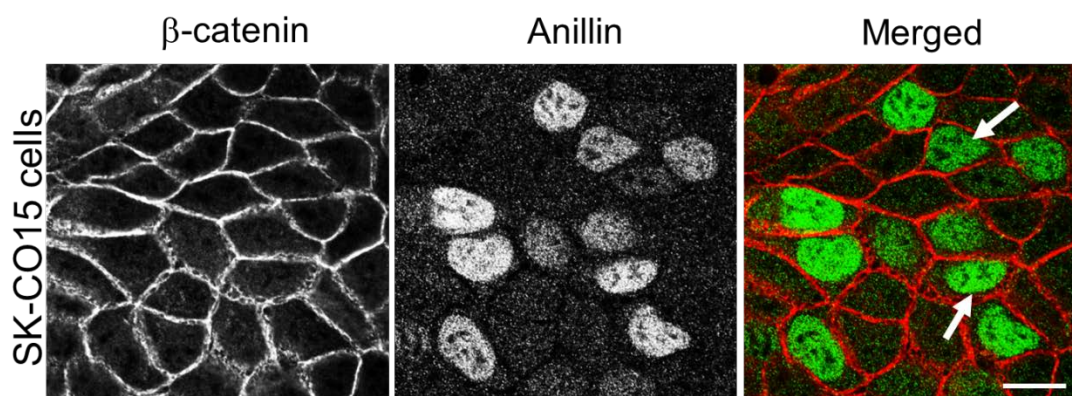
**Suppl. Fig. 1 Anillin depletion disrupts AJ and TJ integrity in different epithelial cell lines.** (a) A549 lung epithelial cells and SK-CO15 colonic epithelial cells were transfected with either control or anillin-specific siRNAs. On day 4 post-transfection, the cells were immunolabeled for different AJ/TJ proteins (a) and the barrier integrity of SK-CO15 cell monolayers was determined using TEER measurement (b). Arrows indicate accumulation of junctional proteins at areas of cell-cell contact in control cells. Arrowheads highlight the disappearance of AJ/TJ proteins from intercellular junctions after anillin depletion. Data is presented as mean  $\pm$  SE (n = 3); \*p < 0.05. Scale bar, 20  $\mu$ m

## Suppl. Fig. 2



**Suppl. Fig. 2 Anillin depletion does not affect expression of different AJ and TJ proteins.** The figure shows immunoblotting analysis of AJ/TJ protein expression in total cell lysates collected from control and anillin-depleted DU145 cells on day 4 post-siRNA transfection

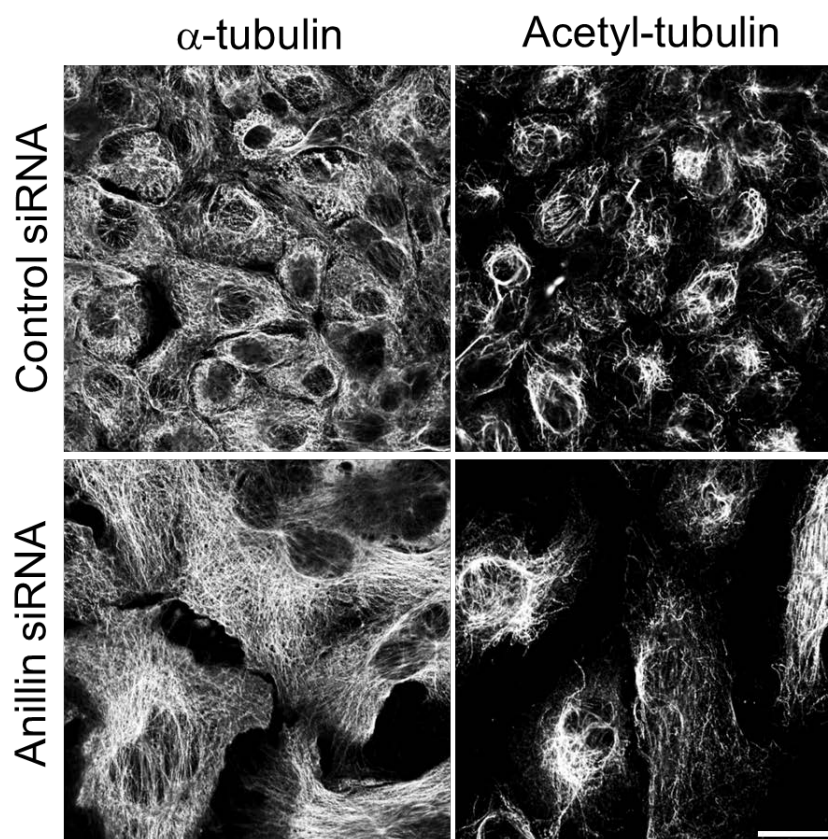
## Suppl. Fig. 3



**Suppl. Fig. 3 Nuclear localization of anillin in human colonic SK-CO15 cell monolayers.**

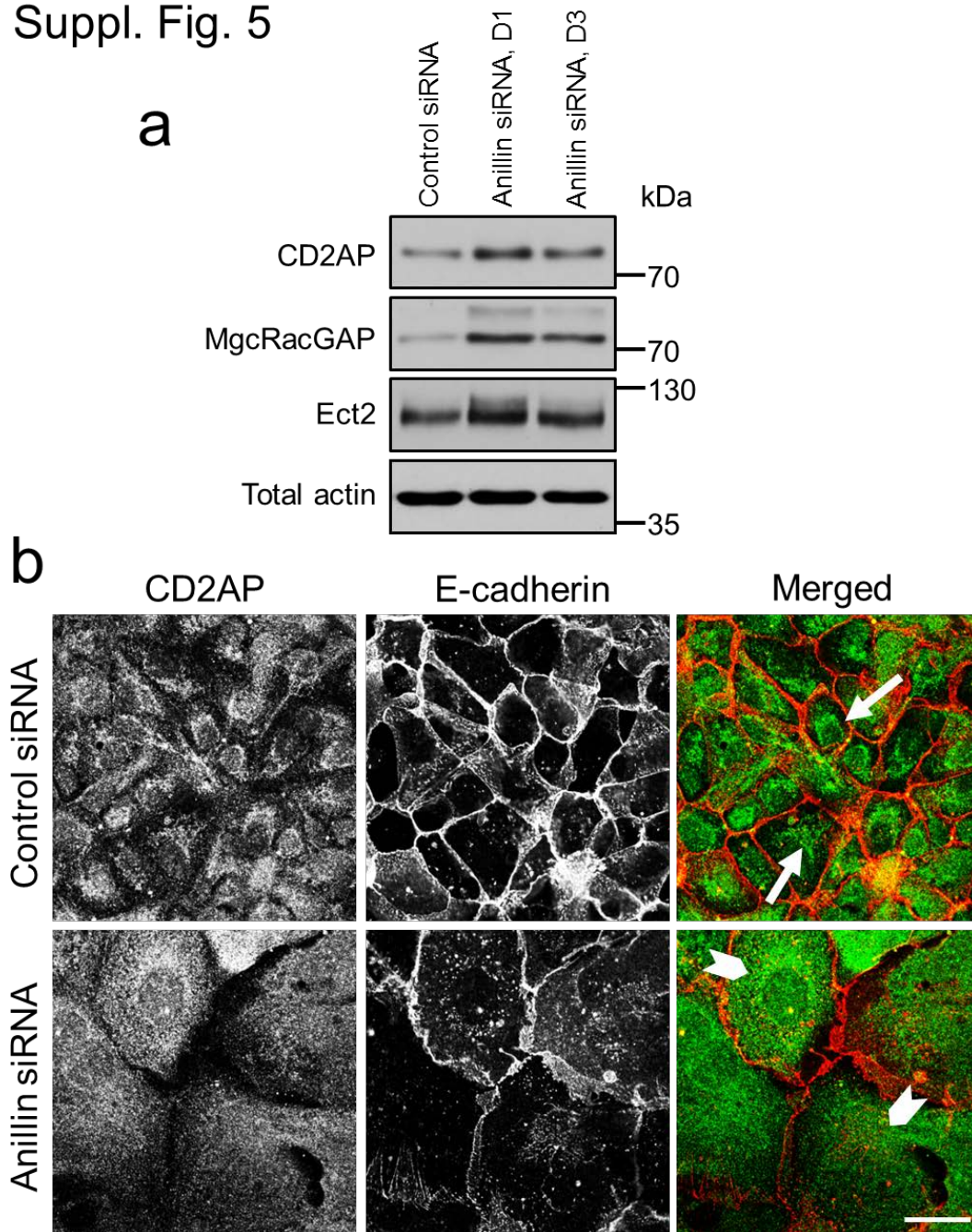
Well-differentiated SK-CO15 cell monolayers were subjected to dual immunolabeling for anillin (green) and  $\beta$ -catenin (red). Arrows indicate specific nuclear localization of anillin. Scale bar, 20  $\mu$ m

## Suppl. Fig. 4

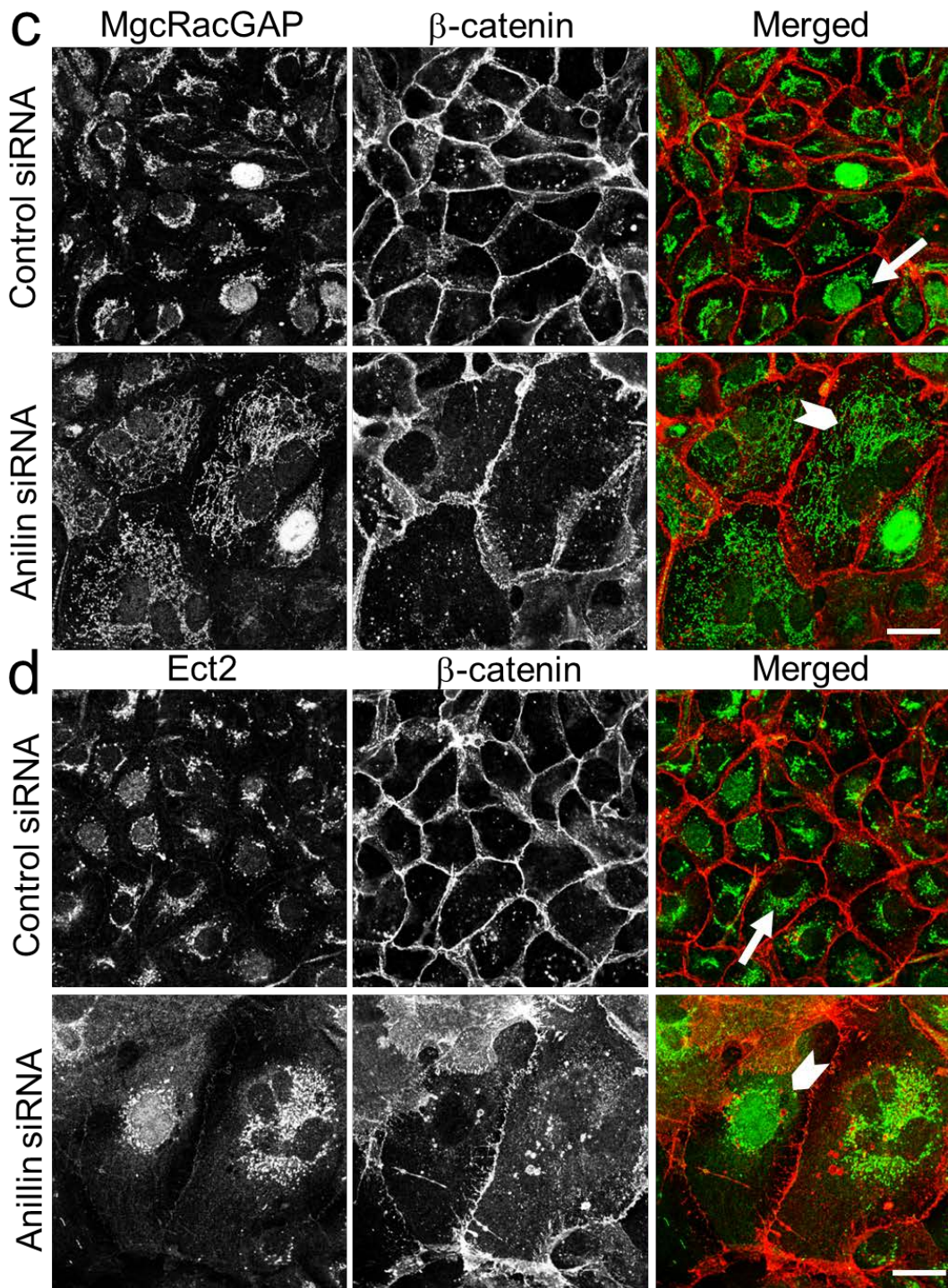


**Suppl. Fig. 4 Loss of anillin does not affect the microtubule cytoskeleton.** DU145 cells transfected with either control or anillin-specific siRNAs were immunolabeled for total and stable microtubules using monoclonal antibodies against  $\alpha$ -tubulin and acetylated tubulin, respectively. Scale bar, 20  $\mu$ m

Suppl. Fig. 5



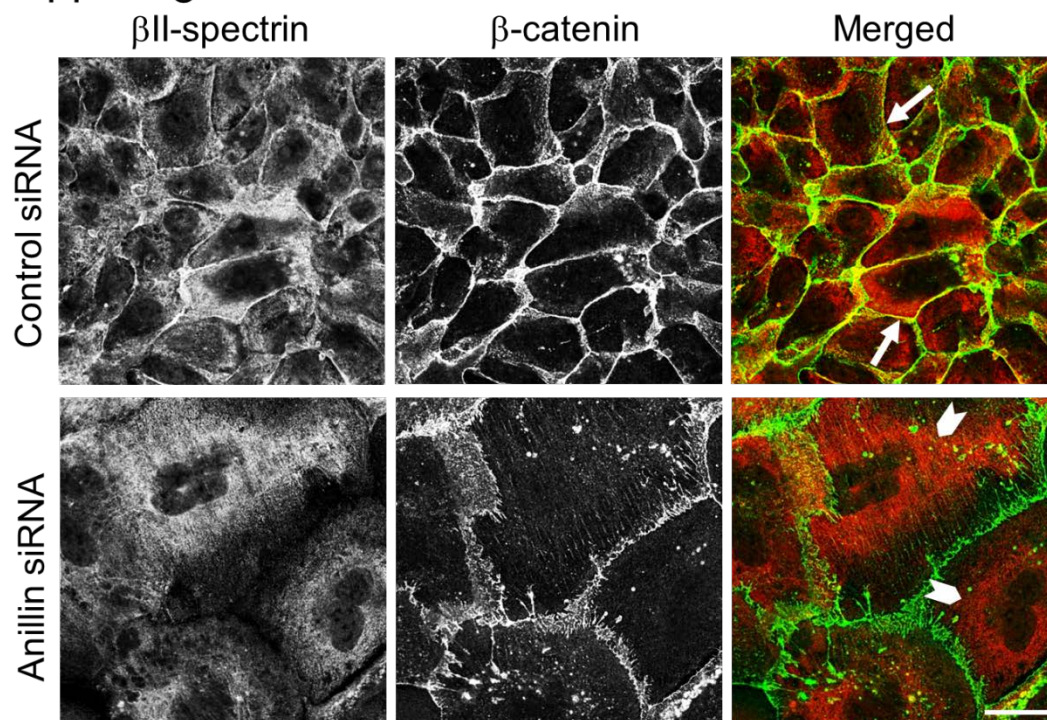
## Suppl. Fig. 5



**Suppl. Fig. 5** Effects of anillin depletion on the expression and localization of its known binding partners that regulate the actin cytoskeleton. (a) Expression of CD2AP, MgcRacGAP and Ect2 was examined in control and anillin-depleted Du145 cells on day 4 post siRNA transfection. (b-d) The effect of anillin knockdown on localization of CD2AP, MgcRacGAP and Ect2 was determined by

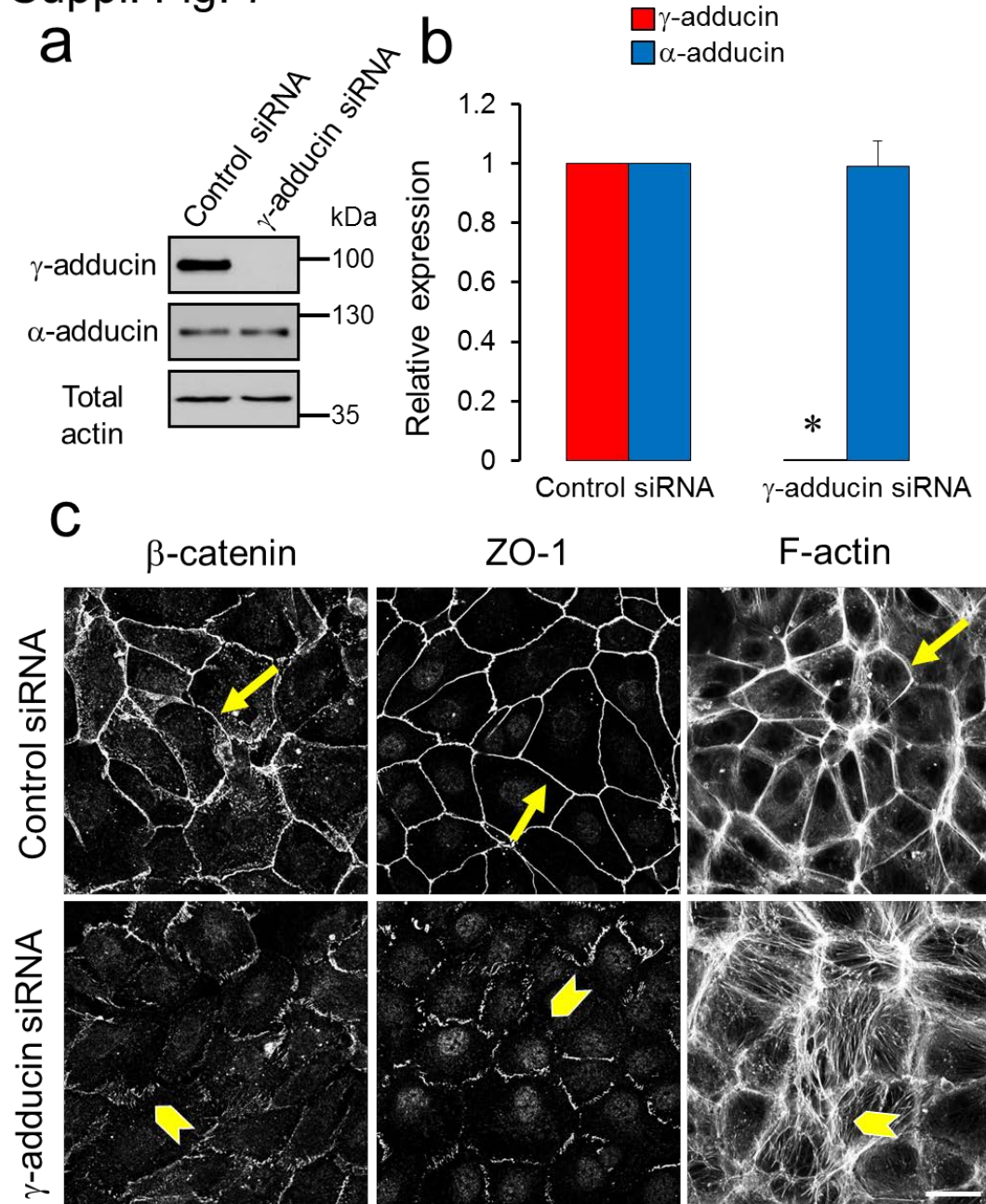
immunofluorescence labeling. Arrows and arrowheads indicate perinuclear accumulation of these proteins in control and anillin-depleted cells, respectively. Scale bar, 20  $\mu\text{m}$

### Suppl. Fig. 6



**Suppl. Fig. 6 Anillin depletion affects cellular distribution of  $\beta$ -spectrin.** DU145 cells were transfected with either control or anillin-specific siRNAs and subjected to dual immunolabeling for  $\beta$ -spectrin (red) and  $\beta$ -catenin (green). Arrows indicate localization of  $\beta$ -spectrin at intercellular junctions in control cells. Arrowheads highlight predominantly cytoplasmic labeling of  $\beta$ -spectrin in anillin-depleted cells. Scale bar, 20  $\mu\text{m}$

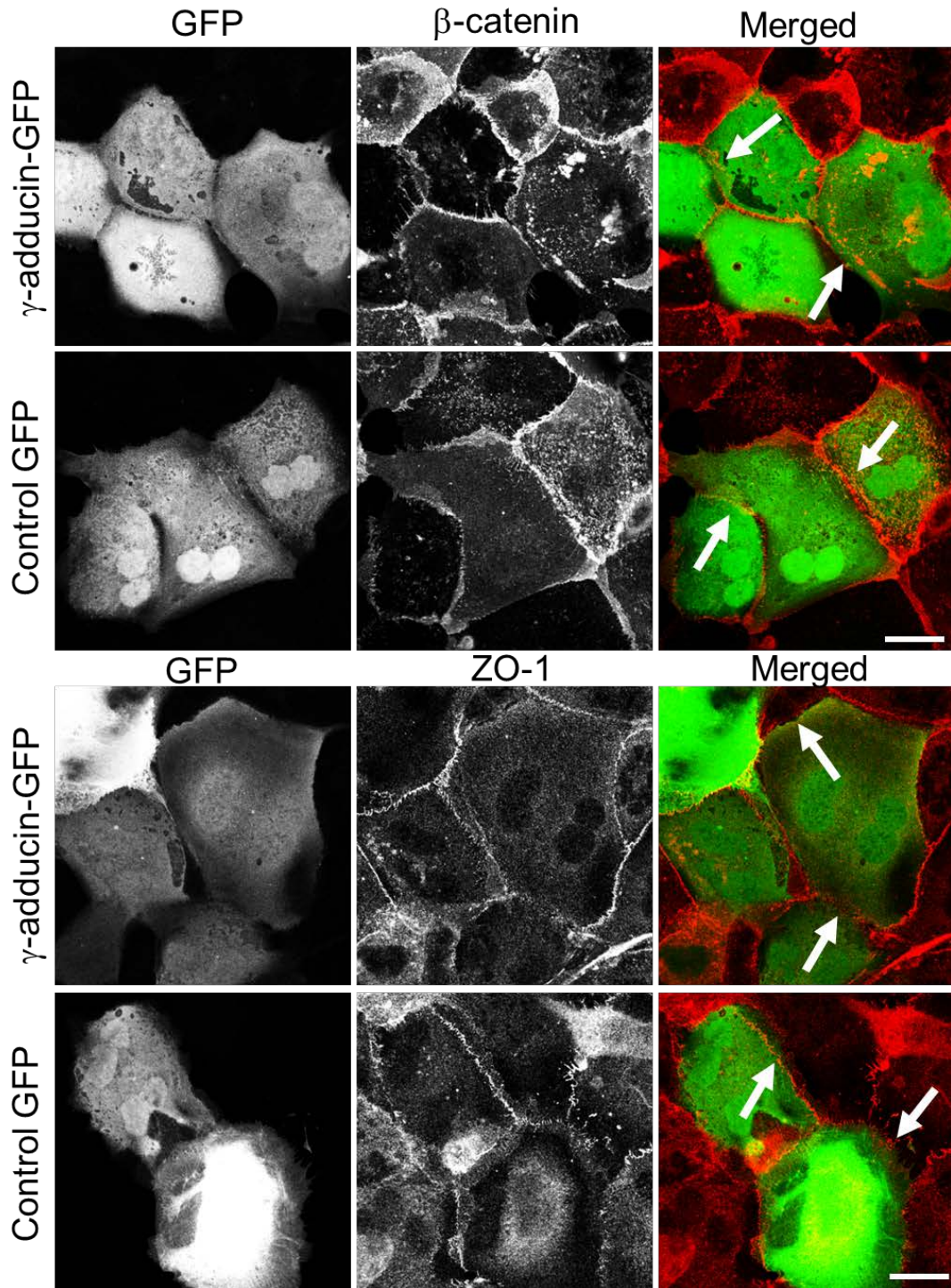
## Suppl. Fig. 7



**Suppl. Fig. 7 Knockdown of  $\gamma$ -adducin disrupts apical junctions and the perijunctional F-actin belt.** (a, b) DU145 cells were transfected with either control or  $\gamma$ -adducin-specific siRNA. The effect of this knockdown on the expression of adducin isoforms was determined by immunoblotting and quantitative densitometric analysis. (c) The integrity of apical junctions and the perijunctional actin cytoskeleton in control  $\gamma$ -adducin-depleted cells was examined by fluorescence labeling. Arrows indicate the intact morphology of AJ, TJ, and circumferential F-actin belt in control cells. Arrowheads

highlight the fragmented, discontinuous intercellular junctions, and disorganized perijunctional F-actin bundles, found after  $\gamma$ -adducin depletion. Scale bar, 20  $\mu$ m

## Suppl. Fig. 8



**Suppl. Fig. 8 Overexpression of  $\gamma$ -adducin does not rescue defects of adherens and tight junctions in anillin depleted epithelial cell.** DU145 cells were co-transfected with anillin-specific siRNAs and

either GFP- $\gamma$ -adducin plasmid or control GFP. Cells were counterstained for either  $\beta$ -catenin or ZO-1 (red) to visualize AJ and TJ. Arrows demonstrate that either GFP- $\gamma$ -adducin or control GFP expression failed to restore junctional integrity in anillin-depleted epithelial cells. Scale bar, 20  $\mu$ m